Bioorganic & Medicinal Chemistry Letters 18 (2008) 6562–6567

Contents lists available at ScienceDirect

Bioorganic & Medicinal Chemistry Letters

journal homepage: www.elsevier.com/locate/bmcl

Succinyl hydroxamates as potent and selective non-peptidic inhibitors of procollagen C-proteinase: Design, synthesis, and evaluation as topically applied, dermal anti-scarring agents

Simon Bailey [a,†,*], Paul V. Fish [a,*], Stephane Billotte [a], Jon Bordner [e], Doris Greiling [b], Kim James [a], Andrew McElroy [a], James E. Mills [a], Charlotte Reed [c], Robert Webster [d]

[a] Department of Discovery Chemistry, Pfizer Global Research and Development, Sandwich Laboratories, Ramsgate Road, Sandwich, Kent CT13 9NJ, UK
[b] Department of Discovery Biology, Pfizer Global Research and Development, Sandwich Laboratories, Ramsgate Road, Sandwich, Kent CT13 9NJ, UK
[c] Department of Pharmaceutical Sciences, Pfizer Global Research and Development, Sandwich Laboratories, Ramsgate Road, Sandwich, Kent CT13 9NJ, UK
[d] Department of Pharmacokinetics, Dynamics & Metabolism, Pfizer Global Research and Development, Sandwich Laboratories, Ramsgate Road, Sandwich, Kent CT13 9NJ, UK
[e] Department of Materials Science, Pfizer Global Research and Development, Groton Laboratories, Eastern Point Road, Groton, CT 06340, USA

ARTICLE INFO

Article history:
Received 19 September 2008
Revised 7 October 2008
Accepted 8 October 2008
Available online 11 October 2008

Keywords:
Succinyl hydroxamates
Procollagen C-proteinase
Transepidermal delivery
Anti-scarring
Conformational analysis

ABSTRACT

Succinyl hydroxamates **1** and **2** are disclosed as novel series of potent and selective inhibitors of procollagen C-proteinase (PCP) which may have potential as anti-fibrotic agents. Carboxamide **7** demonstrated good PCP inhibition and had excellent selectivity over MMPs involved in wound healing. In addition, **7** was effective in a cell-based model of collagen deposition (fibroplasia model) and was very effective at penetrating human skin in vitro. Compound **7** (UK-383,367) was selected as a candidate for evaluation in clinical studies as a topically applied, dermal anti-scarring agent.

Fibrosis is a complex process which is characterized by excessive accumulation of extracellular matrix (ECM), principally type I collagen.[1,2] In the case of wounds to the skin, dermal fibroblasts respond to activation by transforming growth factor-β (TGF-β1) by releasing soluble procollagens and procollagen C-proteinase (PCP; EC 3.4.24.19 also known as BMP-1).[3–5] Proteolytic cleavage of the C-terminal propeptide of types I, II, and III procollagens by PCP affords collagen, which undergoes self-assembly into fibrils followed by cross-linking to give an insoluble collagen matrix. The excessive accumulation of ECM by these processes leads to the formation of scar tissue.[6] Hence, inhibition of PCP activity[7] was identified as an attractive point at which to intervene in the collagen deposition pathway.

In this letter, we now describe the detailed SAR which lead to the identification and optimization of oxadiazoles **1** and oxazoles **2** as potent and selective non-peptidic inhibitors of PCP. Furthermore, one of these compounds, **7** (UK-383,367) was selected as a candidate for clinical evaluation as a *topically* applied, dermal anti-scarring agent.[8]

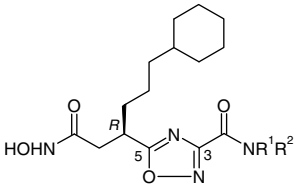

1

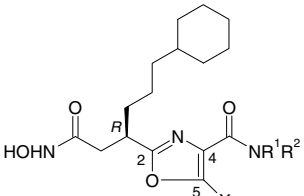

2

Previously, we have described the identification of the succinyl hydroxamate template by a combination of file screening of libraries of matrix metalloproteinase (MMP) inhibitors and specific structural modifications; these efforts furnished oxadiazole ester **6** as a starting point for optimization (Fig. 1).[8,9] Although it was clear that the lipophilic side chain of **6** played an important role in regulating activity against PCP (compare **3** vs **4** and **5** vs **6**), it was decided to explore replacements for the chemically and metabolically vulnerable C3-ester group in the first phase of analogue synthesis. In particular, the effect of simple carboxamide substitu-

* Corresponding authors. Tel.: +1 858 526 4692 (S.B.); tel.: +44 (0)1304 644589 (P.V.F.).
E-mail addresses: simon.bailey@pfizer.com (S.B.), paul.fish@pfizer.com (P.V.F.).
† Present address: Department of Chemistry, Pfizer Global R & D, La Jolla Labs, San Diego, CA 92121, USA.

0960-894X/$ - see front matter © 2008 Elsevier Ltd. All rights reserved.
doi:10.1016/j.bmcl.2008.10.036

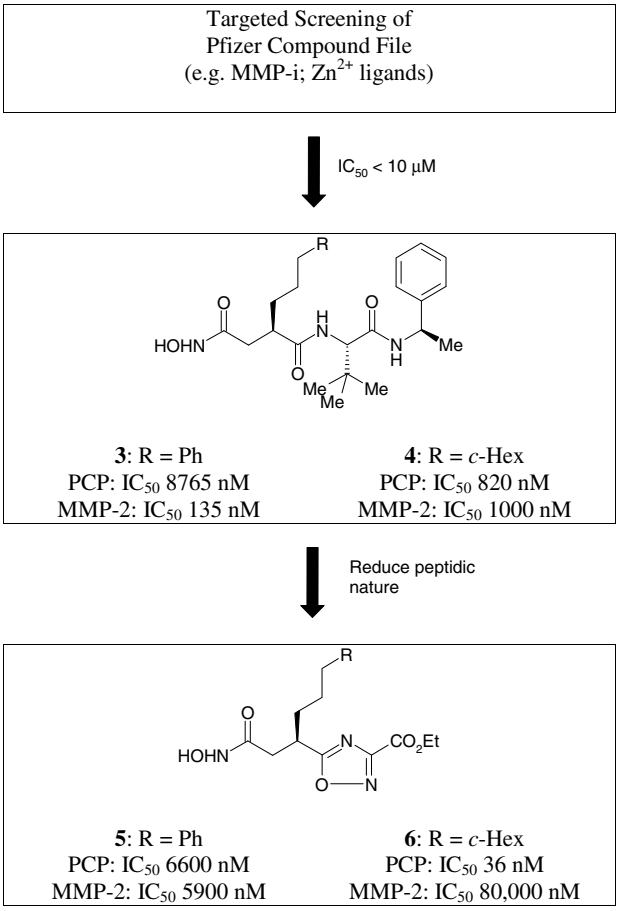

Figure 1. Summary of key structures in the identification of succinyl hydroxamate lead series by a combination of file screening and specific structural modifications.

ents on the oxadiazole ring was assessed, and, as an initial venture –$CONH_2$ (**7**), –CONHMe (**8**), and –$CONMe_2$ (**9**) were prepared and screened for inhibition of PCP activity.

These carboxamides furnished promising leads as **7**–**9** all had PCP inhibitory activity equivalent or superior to ester **6** and no significant MMP-2 activity (Table 1). *tert*-Amide **9** was the most potent inhibitor (IC_{50} 10 nM) of this set and gave encouragement that potent, selective inhibitors of PCP could be achieved. Hence, a more detailed investigation of the SAR of the carboxamide substituent was undertaken in both the oxadiazole (**1**) and oxazole (**2**) templates.

The synthesis of oxadiazole target compounds **7**–**21** (Table 1) were prepared as described in Scheme 1. *N*-Hydroxy amidine **27** was coupled with (*R*)-succinic acid mono-ester **26**[10] to give the *O*-acyl derivative **28** and then thermal cyclodehydration of **28** in xylene created the 1,2,4-oxadiazoles **29**. Two general methods were used to install the 3-carboxamide: either selective deprotection of the *tert*-butyl esters with TFA gave carboxylic acid **30** and then treatment with amines HNR^1R^2 gave amides **31**, or alternatively, these two steps were reversed (i.e., **29** → **32** → **31**). Finally, activation of the carboxylic acid **31** with *i*-BuOCOCl followed by reaction with $TMSONH_2$ and methanolic work-up afforded hydroxamates **7**–**21**. The (*S*)-enantiomer (*S*)-**7** was prepared by an identical sequence but starting with (*S*)-**26**.

The oxazoles target compounds **22**–**25** (Table 2) were prepared using a similar overall synthetic strategy as for the oxadiazoles but employed the methods of Wipf[11] for the creation of the oxazole ring (Scheme 2). (*R*)-Succinic acid mono-ester **26** was esterified with an appropriate L-serine (**33**) or L-threonine (**34**) derivative

Table 1
PCP and MMP-2 inhibition by oxadiazole carboxamides **7–21**[a,b]

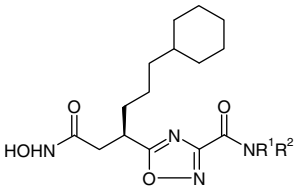

7-21

Compound	NR^1R^2	PCP IC_{50} (nM)	MMP-2 IC_{50} (nM)
7	NH_2	44	>60,000
(*S*)-**7**	NH_2	>2000	NT
8	NHMe	28	>30,000
9	NMe_2	10	>100,000
10	NH-nPr	32	21,700
11	NH-*i*-Pr	21	>100,000
12	$NHCH_2$-cPr	33	>30,000
13	$NHCH_2Ph$	57	NT
14	$NHCH_2$(2-Py)	37	>30,000
15	$NHCH_2CO_2H$	21	>100,000
16	Pyrrolidine	43	NT
17	Piperidine	26	74,900
18	Morpholine	25	NT
19	4-Methylpiperazine	54	NT
20	$N(Me)CH_2Ph$	65	81,800
21	$N(Me)CH_2$(2-Py)	40	50,500

[a] See Ref. 9 for complete details of assay conditions. IC_{50} values are geometric means of at least three experiments. Differences of <2-fold should not be considered significant.
[b] NT denotes not tested.

to afford the alcohols **35** and **36**, respectively. Reaction of serine-derived alcohol **35** with the Burgess reagent promoted cyclodehydration to oxazoline **37**, which then underwent aromatization to the corresponding oxazole by treatment with $CuBr_2$/DBU.[12] At this point, a protected hydroxamic acid group was introduced to give **38** prior to hydrolysis of the ethyl ester and amide formation under standard conditions. Finally, the hydroxamate benzyl protecting group was cleaved by hydrogenolysis to give **22** and **23**. A different order of chemical steps was employed for the fully substituted 5-Me-oxazole targets **24**–**25**. Oxidation of the secondary alcohol **36** using the Dess–Martin reagent gave the keto-amide **39** which underwent ring closure by the action of PPh_3-I_2 to afford **40**[13] Oxazole **40** was converted to the targets **24**–**25** using transformations similar to those described above.

All target compounds (Tables 1 and 2) were tested for their ability to inhibit the PCP mediated cleavage of a fluorogenic peptide substrate.[14] Selected compounds were then routinely assessed for physicochemical properties consistent with transepidermal delivery (TED)[15] (mp > 110 °C; aq solubility > 50 μg/ml; stability under autoclave conditions), and for selectivity over MMPs involved in wound healing.[16] Inhibition of PCP activity was confirmed for selected compounds with the endogenous substrate procollagen. Finally, preferred compounds were evaluated in an in vitro cell-based model of collagen deposition (fibroplasia model)[17] and for their ability to penetrate human skin in vitro.[18]

A wide variety of amide substituents were tolerated at the C-3 position of the oxadiazole (Table 1). Thus, the primary amide **7**, *n*-alkyl secondary amides **8** and **10**, as well as those with branching at the α- or β-carbon, **11** and **12**, respectively, all inhibit PCP with IC_{50}s in the 20–45 nM range. The benzylamide, **13**, does show a small, 2-fold, drop in potency compared with the methyl amide **8**. However, activity is largely restored when a heteroaryl ring is featured as in compound **14**. The presence of a carboxylic acid group, as in **15**, did not detrimentally influence activity.

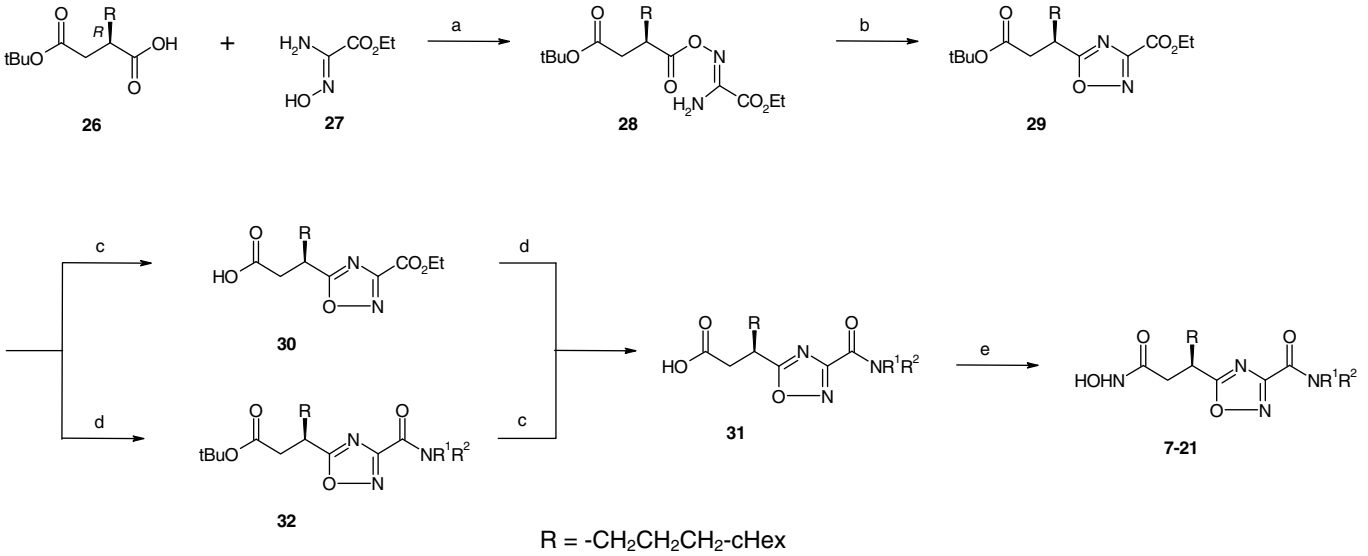

Scheme 1. Synthesis of oxadiazole 3-carboxamides **7**–**21**. Reagents and conditions: (a) WSCDI, HOBt, 1,4-dioxane, 0 °C → rt; (b) xylene, 130 °C; (c) TFA, CH_2Cl_2, 0 °C → rt; (d) HNR^1R^2, EtOH; (e) *i*-BuOCOCl, *N*-methylmorpholine, THF or DMF, 0 °C, then $H_2NOSiMe_3$, rt, then MeOH, rt.

A similar pattern was observed with tertiary amides **16**–**21**, with acyclic and cyclic moieties all having relatively little influence on enzyme inhibition. The presence of heteroatoms **18**, and basic centers **19** were well tolerated with only minor variations in the observed potencies. Again, the incorporation of a benzyl group **20** gives rise to slightly weaker activity than that seen with other moieties. Hence, it has proved difficult to improve PCP inhibitory activity below a plateau of IC_{50} < 20–45 nM.

It is of note that the absolute stereochemistry of chiral center had a profound effect on PCP activity with the (*R*)-enantiomer being superior (e.g., (*R*)-**7** vs (*S*)-**7**). Furthermore, no compound had any significant inhibition of MMP-2 activity providing evidence that the 6-cyclohexyl-*N*-hydroxyhexanamide backbone confers good affinity for PCP and selectivity over MMP-2.

For the PCP inhibitors in Table 1, it was expected that the C3 amide group and the 1,2,4-oxadiazole ring would lie co-planar due to favorable mesomeric stabilization. As a consequence, there would be barriers to free rotation of the amide substituent about the carbonyl-heterocycle bond. In contrast, it was expected that a carboxamide directly attached at C4 of a 1,3-oxazole ring might allow additional favorable binding modes to become available. The oxazole ring would allow the incorporation of a H- or Me-substituent at C5 and promote an out-of-plane conformation of the amide through alleviation of steric congestion. Consequently, the oxazoles **22**–**25** were prepared and screened for inhibition of PCP activity (Table 2).

Table 2
PCP inhibition by oxazole carboxamides **22**–**25**

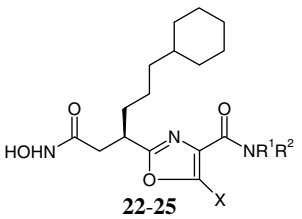

Compound	NR^1R^2	X	PCP IC_{50} (nM)
22	NH_2	H	73
23	NMe_2	H	45
24	NH_2	Me	17
25	NMe_2	Me	17

Comparison of PCP activity of C5-H oxazoles, **22** and **23**, with the corresponding oxadiazole analogues, **7** and **9**, shows that activity is largely retained in the oxazole series but with a slight loss in activity. In contrast, the C5-Me substituted oxazoles, **24** and **25**, are amongst the most potent PCP inhibitors identified in the carboxamide series.

These results prompted a more detailed analysis of the preferred conformation of the heterocycle-amide bond. Torsion angle calculations predicted **7**, **22**, and **24** would all have a preference for an in-plane conformation (Fig. 2) and these calculations were supported by a single crystal X-ray structure determination of **7** monohydrate which also showed a planar arrangement of the carboxamide and oxadiazole ring (Fig. 3).[19,20] These results were somewhat unexpected, and the observations/principles may prove to have general utility in the design of azole derivatives. Hence we concluded that the slight increase in affinity for **24** (and **25**) was due to an additional positive binding interaction between the C5-Me and the protein structure rather than conformational effects.

Overall the data presented in Tables 1 and 2 indicated that the contribution to PCP binding affinity provided by the heterocycle and the carboxamide substituent was relatively minor and, consequently, this amide position proved to be a good handle for tuning the physicochemical properties.

From these experiments, primary amide **7** emerged as having a superior combination of PCP activity (IC_{50} 44 nM) combined with selectivity over MMP-2 (>1000-fold) and physicochemical properties thought suitable for TED delivery, and so was selected for further assessment.

Inhibition of PCP enzymatic activity was confirmed as amide **7** was found to inhibit the turnover of procollagen with a slightly enhanced potency (IC_{50} 26 nM) (Table 3). Additional screening of **7** against a panel of MMPs showed no significant activity (IC_{50} > 10,000 nM) (Table 3).

Amide **7** was then assessed for its potential to block collagen deposition in an in vitro fibroplasia model (Table 3).[17] After culturing human dermal fibroblasts for 8 days, **7** showed a dose-dependant reduction in collagen deposition, both by histological analysis and by quantification of hydroxyproline content. From the quantitative hydroxyproline analysis, **7** inhibited collagen

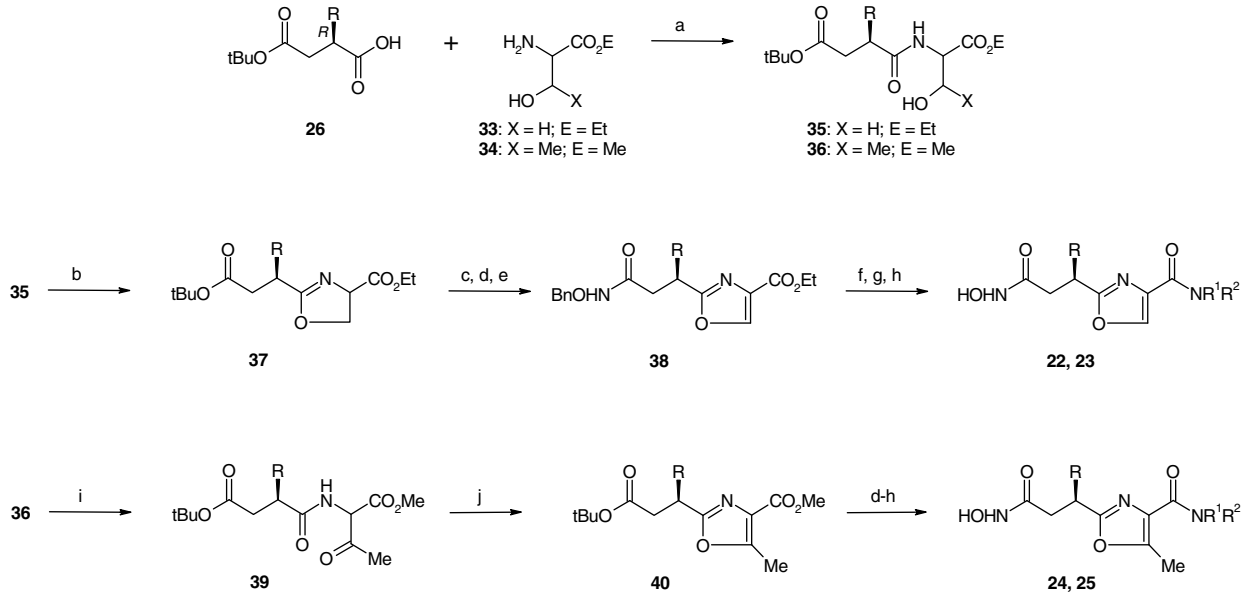

Scheme 2. Synthesis of oxazole 4-carboxamides **22**–**25**. Reagents and conditions: (a) WSCDI, HOBt, *i*-Pr_2NEt, CH_2Cl_2, 0 °C → rt; (b) Burgess reagent, THF, 80 °C; (c) $CuBr_2$, DBU, HMTA, CH_2Cl_2, 0 °C → rt; (d) TFA, CH_2Cl_2, 0 °C → rt; (e) $BnONH_2$, CDI, *i*-Pr_2NEt, THF, rt; (f) LiOH, 1,4-dioxane-H_2O, 0 °C; (g) HNR^1R^2, WSCDI, HOBt, *N*-methylmorpholine, CH_2Cl_2, rt; (h) 5% Pd-$BaSO_4$, H_2 or $NH_4^+HCO_2^-$, EtOH; (i) Dess–Martin periodinane, CH_2Cl_2, rt; (j) I_2, PPh_3, NEt_3, THF, −78 °C → 0 °C.

deposition by >70% at 10 μM and with an IC_{50} of approximately 2 μM.

The ability of **7** to penetrate human skin in vitro was measured using standard transdermal assays. Human cadaver stratum corneum was mounted in a Franz diffusion cell and exposed to a solution of **7** in 50% aqueous propylene glycol for 24 h. The concentration of **7** passing through the skin to a receptor chamber was measured and used to calculate a TED flux rate (Table 3). Encouragingly, in this system **7** permeated through the skin with a calculated flux value of 0.30 ± 0.09 μg/cm^2/h which compared favorably with values for agents which are known to penetrate skin well in vivo.[21] A more detailed analysis of the ability of **7** to penetrate human skin was then performed. When propylene glycol–citrate buffer–ethanol (20:30:50) was employed as the TED vehicle, the saturated solubility increased to 13,800 μg/ml and the TED flux increased to 1.59 ± 0.56 μg/cm^2/h.

Compound **7** was screened for off-target pharmacology against a panel of receptors, enzymes and ion channels and was found to have modest binding affinity for only the PDE-4 enzyme (69% inhibition at 10 μM; non-subtype specific). Further evaluation showed **7** to have modest affinity for all the PDE-4 subtypes [IC_{50} (μM): PDE-4a = 1.8; 4b = 1.5; 4c = 2.4; 4d = 0.9]. The consequences of this weak PDE-4 activity was not clear although PDE-4 inhibition has been shown to attenuate TGF-β mediated pro-collagen synthesis and can also be considered a potential anti-fibrotic target.[22]

In the context of treating dermal scarring by TED delivery, it was felt that a compound with low systemic exposure would

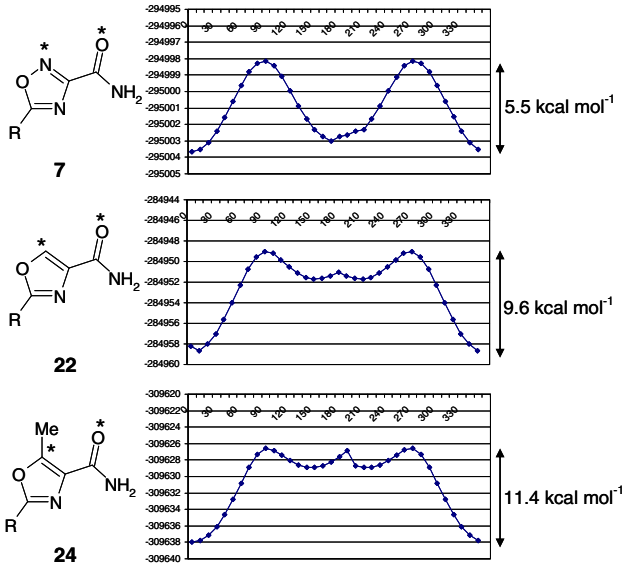

Figure 2. Torsion angle scan energy calculations of **7**, **22**, and **24** to illustrate the lowest energy conformations of the carboxamide wrt the heterocycle. The lowest energy structures are shown; the * indicating the atoms for which the torsion angle was measured. The calculations were carried out using Density Functional Theory at B3LYP/6-31G** level of theory (Jaguar v6.5).

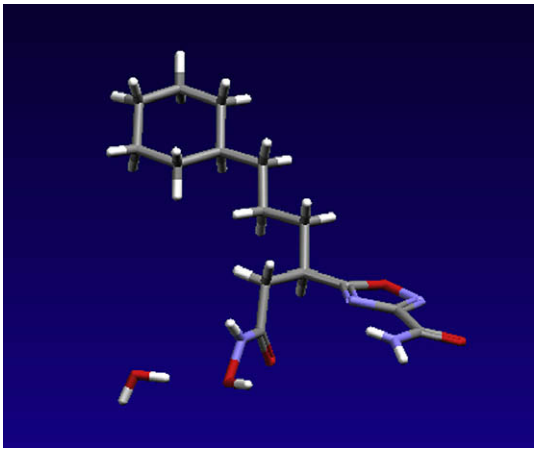

Figure 3. Single crystal X-ray structure determination of **7** monohydrate which shows a planar arrangement of the 3-carboxamide and 1,2,4-oxadiazole ring.

Table 3
Summary of physicochemical properties, MMP selectivity, efficacy in the fibroplasia model and ability to penetrate human skin for compounds **7** and **9**[a,b]

	7	**9**
Physicochemical properties:		
Mw	324	352
Log $D_{7.4}$	2.6	3.6
pK_a	9.0	NT[c]
Mp (°C)	136–138	Oil
Satd aqueous solubility in PBS (pH 7.4) (μg/ml)	35	900
PCP activity:		
Peptide substrate, IC_{50} (nM)	44	10
[^{3}H]-procollagen, IC_{50} (nM)	26	9.3
MMP selectivity:		
MMP-1, IC_{50} (nM)	>10,000	NT
MMP-2, IC_{50} (nM)	>60,000	>100,000
MMP-3, IC_{50} (nM)	>10,000	28,000
MMP-9, IC_{50} (nM)	>10,000	NT
MMP-14, IC_{50} (nM)	>10,000	NT
Efficacy in the fibroplasia model:[d]		
% I @ 10 μM	76 ± 5	67 ± 14
IC_{50} (nM)	2100 ± 500	NT
In vitro penetration through human skin in 50% aqueous propylene glycol (pH 6.8):[e]		
Solubility, C_o (μg/ml)	670	8260
TED flux (μg/cm^2/h)	0.30 ± 0.09	2.6 ± 1.6

[a] See Ref. 9 for complete details of assay conditions.
[b] NT denotes not tested.
[c] pK_a ~ 9.0 by analogy with the measured value for **7**.
[d] Mean ± SEM ($n \geqslant 4$).
[e] Mean ± SEM (n = 6–10).

Table 4
Pharmacokinetic parameters of **7** after single intravenous and oral administration to rat and dog[a]

	Male rat (n = 2)	Male dog (n = 2)
Intravenous dose (mg/kg)	2	0.5
Elimination half-life, $T_{1/2}$ (h)	0.8	1.5
Plasma clearance, Cl (ml/min/kg)	157	35
Volume of distribution, V_d (l/kg)	12	4.6
Oral dose (mg/kg)	NT	2
C_{max} (ng/ml)	—	110
T_{max} (h)	—	0.5–1.5
Oral bioavailability, F_o (%)	—	13

[a] NT denotes not tested.

minimize any potential safety concerns through any off-target activity. Screening in ADME assays showed **7** to have low stability in liver microsomes [$T_{1/2}$ (min): HLM 19; DLM 9; RLM < 2] consistent with high predicted clearance. Investigation of the primary routes of metabolism in human, dog, and rat microsomes suggested **7** was primarily metabolized at the hydroxamate group to yield the corresponding carboxylic acid and primary carboxamide. These metabolites were not inhibitors of PCP activity (IC_{50} > 30 μM).

Pharmacokinetic data for **7** were generated in vivo in rat and dog following intravenous and oral administration (Table 4).[23] Following single intravenous administration to rat, the plasma clearance of **7** was high (Cl 157 ml/min/kg) resulting in an elimination half-life of 0.8 h. Concentrations were below the limit of quantification (<0.1 μg/ml) after 2 h post-administration of the dose. Plasma clearance in dog was lower than that observed in rat but still high relative to liver blood flow. The oral bioavailability of **7** in dog was low (13%) in keeping with the plasma clearance observed. Following administration of **7** to the isolated perfused rat liver a hepatic extraction rate of 75–86% was obtained, suggesting that **7** undergoes extensive hepatic clearance. These results would predict rapid systemic clearance following TED delivery.

Topical pharmacokinetics in vivo confirmed **7**, dosed as a solution of 0.9 mg/ml in 50% aqueous propylene glycol, penetrated intact pig skin with tissue levels in the upper dermis reaching a steady state concentration of 10 μM after 24 h. Furthermore, no systemic exposure of **7** was detected following topical administration in this model following repeat dosing over 7 days.

N,*N*-Dimethyl amide **9** was the most potent PCP inhibitor (IC_{50}10 nM) of this set and was also selected for further characterization (Table 3). Amide **9** was comparable to **7** in nearly all parameters except that it lacked a suitable crystalline solid form. Although not appropriate for potential clinical use, **9** proved to be valuable tool in the development of preclinical models of scarring. Evaluation of **9** in a rabbit model of cutaneous scarring established that inhibition of PCP in vivo reduces scar hypertrophy.[24] These results support the potential use of PCP inhibitors to mitigate hypertrophic scarring.

In summary, succinyl hydroxamates **1** and **2** are disclosed as novel series of potent and selective inhibitors of PCP which may have potential as anti-fibrotic agents. Compound **7** demonstrated good PCP inhibition and had excellent selectivity over MMPs involved in wound healing. In addition, **7** was effective in a cell-based model of collagen deposition (fibroplasia model) and was very effective at penetrating human skin in vitro. Furthermore, compound **9** (UK-369,930), a close relative to **7** in terms of both structure and profile, reduced scar hypertrophy in a rabbit model of scarring. Based on this information, **7** (UK-383,367) was selected as a candidate for evaluation in clinical studies as a topically applied, dermal anti-scarring agent. The results of these studies will be reported in future publications.

Acknowledgments

We thank the following colleagues for their expert and enthusiastic technical assistance: Lyndsey Addison, Yvonne Ailwood, Cathy Allan, Gillian Allan, Gerwyn Bish, Usa Datta, Vikki Dawe, Samantha Gaboardi, John Harvey, Carol Loosley, Emma Newstead, Julie Owen, Christelle Pasquinet, Clint Pereira, and Simon Planken.

In addition we acknowledge the excellent support of the Physical Sciences group.

References and notes

1. Trojanowska, M.; LeRoy, E. C.; Eckes, B.; Krieg, T. *J. Mol. Med.* **1998**, *76*, 266.
2. Border, W. A.; Noble, N. A. *NEJM* **1994**, *331*, 1286.
3. Lee, S.; Solow-Corero, D. E.; Kessler, E.; Takahara, K.; Greenspan, D. S. *J. Biol. Chem.* **1997**, *272*, 19059.
4. Kessler, E. In *Procollagen C-Proteinase*. In *The Handbook of Proteolytic Enzymes*; Academic press, 1998. pp 1–5.
5. Kessler, E.; Takahara, T.; Biniamov, L.; Brusel, M.; Greenspan, D. S. *Science* **1996**, *271*, 360.
6. Rhett, J. M.; Ghatnekar, G. S.; Palatinus, J. A.; O'Quinn, M.; Yost, M. J.; Gourdie, R. G. *Trends Biotechnol.* **2008**, *26*, 173.
7. For a review of PCP inhibitors, see: Turtle, E. D.; Ho, W.-B. *Expert Opin. Ther. Patents* **2004**, *14*, 1185.
8. (a) Bailey, S.; Billotte, S.; Derrick, A. M.; Fish, P. V.; James, K.; Thomson, N. M. WO 2001047901.; (b) Bailey, S.; Fish, P. V.; James, K.; McElroy, A. *Abstracts of Papers*, 227th ACS Nation Meeting, Anaheim, CA, March 28–April 1, 2004.
9. Fish, P. V.; Allan, G. A.; Bailey, S.; Blagg, J.; Butt, R.; Collis, M. G.; Greiling, D.; James, K.; Kendall, J.; McElroy, A.; McCleverty, D.; Reed, C.; Webster, R.; Whitlock, G. A. *J. Med. Chem.* **2007**, *50*, 3442.
10. Derrick, A. M.; Thomson, N. M. EP 1199301, 2002.
11. Wipf, P.; Miller, C. P. *Tetrahedron Lett.* **1992**, *33*, 907.
12. Barrish, J. C.; Singh, J.; Spergel, S. H.; Han, W. C.; Kissick, T. P.; Kronenthal, D. R.; Mueller, R. H. *J. Org. Chem.* **1993**, *58*, 4494.
13. Wipf, P.; Miller, C. P. *J. Org. Chem.* **1993**, *58*, 3604.
14. Complete experimental procedures for all assays can be found in Ref. 9.
15. (a) Kasting, G. B.; Smith, R. L.; Cooper, E. R.. In *Pharmacol. Skin*; Karger: Basel, 1987; Vol. 1. p 138; (b) Hadgraft, J.; Valenta, C. *Int. J. Pharm.* **2000**, *200*, 243; (c) Potts, R. O.; Guy, R. H. *Pharm. Res.* **1995**, *12*, 1628.
16. Lijnen, H. R.; Collen, D. *Plasminogen* **2003**, 189.
17. (a) Clark, R. A. F.; McCoy, G. A.; Folkvord, J. M.; McPherson, J. M. *J. Cell. Physiol.* **1997**, *170*, 69; (b) Newstead, E. L.; Gaboardi, S.; Huggins, J. P.; Greiling, D. *J. Dermatol. Sci.* **1998**, *16*(Suppl. 1), S128.
18. (a) Barry, B. W. *Dermatological Formulations in Drugs and the Pharmaceutical Sciences*; Marcel Dekker Inc.: NY, 1983. p 127; (b) Roberts, M. S. Structure–permeability considerations in percutaneous absorption. In *Prediction, of Percutaneous Penetration—Methods, Measurements, and Modelling*; Scott, R. C., Guy, R. H., Hadgraft, J., Bodde, H. E., Eds.; IBC Technical Services, 1991; Vol. 2, p 210.
19. Crystallographic data (excluding structure factors) for **7**•H_2O have been deposited with the Cambridge Crystallographic Data Centre as Supplementary Publication Number CCDC707773. Copies of the data can be obtained free of charge, on application to CCDC, 12 Union Road, Cambridge, CB2 1EZ, UK.
20. An analysis of crystal structures of related compounds available in the PDB and CCDC also showed planar arrangements between the carboxamide and the oxadiazole and oxazole rings.
21. To establish a baseline level of acceptable flux in our in vitro TED model, a set of compounds with commercial precedence of successful transdermal delivery were evaluated, utilizing the same vehicle and test conditions. For example, a solution of clonidine at 1 mg/ml had a TED flux of 0.14 $\mu g/cm^2/h$.
22. (a) Grady, M. W.; Bloor, S. 1999, EP 930069; (b) Duncan, M. R.; Frazier, K. S.; Abramson, S.; Williams, S.; Klapper, H.; Huang, X.; Grotendorst, G. R. *FASEB J.* **1999**, *13*, 1774.
23. Allan, G. A.; Gedge, J. I.; Nedderman, A. N. R.; Roffey, S. J.; Small, H. F.; Webster, R. *Xenobiotica* **2006**, *36*, 399.
24. Reid, R. R.; Mogford, J. E.; Butt, R.; deGiorgio-Miller, A.; Mustoe, T. A. *Wound Rep. Reg.* **2006**, *14*, 138.